Study of Rust Effect on the Corrosion Behavior of Reinforcement Steel Using Impedance Spectroscopy

HAKIM BENSABRA and NOUREDDINE AZZOUZ

Most studies on corrosion of steel reinforcement in concrete are conducted on steel samples with polished surface (free of all oxides) in order to reproduce the same experimental conditions. However, before embedding in concrete, the steel bars are often covered with natural oxides (rust), which are formed during exposure to the atmosphere. The presence of this rust may affect the electrochemical behavior of steel rebar in concrete. In order to understand the effect of rust on the corrosion behavior of reinforcement steel, potentiodynamic and electrochemical impedance spectroscopy (EIS) tests were carried out in a simulated concrete pore solution using steel samples with two different surface conditions: polished and rusted samples. The obtained results have shown that the presence of rust on the steel bar has a negative effect on its corrosion behavior, with or without the presence of chlorides. This detrimental effect can be explained by the fact that the rust provokes a decrease of the electrolyte resistance at the metal-concrete interface and reduces the repassivating ability. In addition, the rust layer acts as a barrier against the hydroxyl ion diffusion, which prevents the realkalinization phenomenon.

DOI: 10.1007/s11661-013-1915-4

I. INTRODUCTION

DEGRADATION of reinforced concrete structures is a matter of great practical importance. Problems are often related to the corrosion of steel reinforcement bars.[1] Under conditions of a good quality concrete, reinforcing steel is normally protected from corrosion by a passive film formed on the steel surface due to the high alkalinity provided by the concrete pore solution (pH > 12.5). However, this passivating environment is not always maintained. It can be modified by two mechanisms: one is chloride ion penetration from the marine environment and the other one is the atmospheric carbon dioxide diffusion.[2–5] The chloride content at the steel-concrete interface is one of the decisive factors for the initiation and propagation of localized corrosion in concrete structures.[6]

Due to the complexity of reinforced concrete systems, simulated concrete pore solutions are usually used in studies of the corrosion behavior of reinforcing steel; most of these are based on KOH, NaOH, and $Ca(OH)_2$, which are all products of cement hydration.[7–12]

The studies on steel corrosion in concrete have most frequently been concentrated on polished steel surface (free of all oxides) in order to reproduce the same experimental conditions. Corrosion products on the surface of steel bars generally exist before the bars are embedded in the concrete. Rust is the most common of these products.

In atmospheric corrosion, steels in ordinary structures, not necessarily in strongly oxidizing environments, corrode to form rust. The rust is generally a coarse, porous, and flaky substance. It has been reported that the main products of rust formed on low alloy steel are α-FeOOH (goethite), β-FeOOH (akaganeite), γ-FeOOH (lipodocrocite), γ-Fe_2O_3 (maghemite), Fe_3O_4 (magnetite), and amorphous hydroxides.[13] The corrosion process of steel bars in atmosphere is affected by both steel chemistry and environmental conditions, namely, duration of exposure, temperature, wet-dry cycles, and the composition of the electrolyte that wets the metal surface.[14,15]

According to the literature, some authors[16,17] reported that the presence of the oxide layers has no significant effect on the corrosion resistance of reinforcement in concrete. Others[18] consider that the presence of oxides on the surface rebar is beneficial, because they act as a physical barrier against aggressive ions. However, most authors[19–24] affirm that the preoxidized steel reinforcements exhibit a high corrosion rate.

To our knowledge, the effect of rust on the reinforcement steel corrosion was well studied using different techniques.[16–23] However, studying this effect by using electrochemical impedance spectroscopy (EIS) has never been reported. Thus, the main objective of this work is to bring up the effect of oxides on reinforcement corrosion resistance in simulated concrete pore solution using EIS.

II. EXPERIMENTAL

A. *Steel and Samples*

The material used was a carbon steel, usually employed in construction. The average chemical composition is given in Table I (all in weight percent).

HAKIM BENSABRA, Ph.D. Candidate, and NOUREDDINE AZZOUZ, Professor, are with the Département de Génie des Procédés, Faculté des Sciences et de la Technologie, Université de Jijel, 18000 Jijel, Algeria. Contact e-mail: hak2dz@yahoo.fr

Manuscript submitted December 9, 2012.
Article published online September 17, 2013

Table I. Chemical Composition of Steel (Weight Percent)

Element	Fe	C	Si	Mn	S	P	Cu	Mo
Percentage	balance	0.12	0.1	0.2	0.02	0.02	0.020	0.06

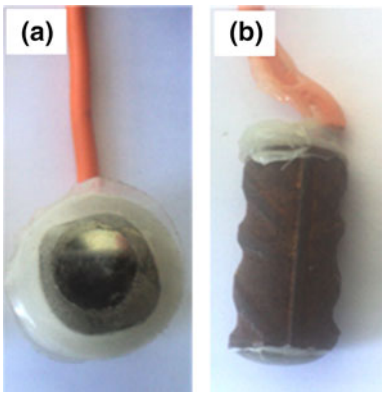

Fig. 1—Steel samples: (*a*) polished sample and (*b*) rusted sample.

To highlight the possible effect of steel surface conditions on the material's corrosion behavior, we have used two different samples (Figure 1):

1. Polished surface samples (reference samples), which were cut from deformed steel bar 10 mm in diameter along the cross section. All of the samples were metallographically polished using a series of silicon carbide emery paper.
2. Rusted samples with 20-mm length (10-mm diameter); in this case, the lateral surface is the active surface (working surface). The samples top and bottom ends were masked with epoxy resin, giving an exposed area of 6.28 cm^2.

B. *Electrolyte*

The electrochemical behavior was analyzed in a saturated $Ca(OH)_2$ solution simulating concrete pore (SCP) solution with pH = 12.5. The solution was prepared with analytical grade reagents and double-distilled water. NaCl concentration of 3 pct was added in the solution in order to simulate the middle of contaminated concrete. A polyethylene cell, suitable for the high alkaline pH of the electrolyte, was employed. All the measurements were carried out at room temperature under aerated conditions and without stirring.

C. *Electrochemical Tests*

The potentiostatic measurements were carried out using a Radio-Meter Analytical potentiostat (PGP201 model) and a cell measuring system with three electrodes: saturated calomel electrode (SCE) as reference electrode, platinum wire as counter electrode, and reinforcement steel as working electrode. Before each test, we measured the free potential after a hold time of 30 minutes; then the polarization curves were plotted in a potential range of –800 to +800 mV_{SCE} with a scanning speed of 0.25 mV s^{-1}.

The electrochemical impedance measurements were performed at frequencies ranging from 10^5 to 10^{-2} Hz using a AC perturbation amplitude of 10 mV around the free potential, measuring 5 points per decade. Zsimp Win software (EChem Software, Ann Arbor, MI) was used for analysis of the EIS spectra. All measurements were performed at room temperature and repeated at least 3 times. Before each measurement, all of the samples were degreased in acetone, rinsed with distilled water, and dried in air.

III. RESULTS AND DISCUSSION

A. *Microstructural Examination*

Metallographic micrographs of polished steel (Figure 2) show two dominant crystalline phases: ferrite and pearlite. The pearlite grains appear darker, while the ferrite is brighter in the micrograph, which is typical microstructure for this alloy. However, we observed a remarkable heterogeneity in the distribution of these two phases: the core material is rich in ferrite, while on board, pearlite is the predominant phase.

This structural heterogeneity has a direct effect on the physicochemical and mechanical properties of steel; mechanically, pearlite, which consists of alternating layers of ferrite and cementite (iron carbides), is harder than ferrite, which gives the steel a compromise of superficial hardness and ductility in the core. In terms of electrochemical behavior, the ferrite is more resistant to corrosion than pearlite; this is due to the fact that pearlite is formed at cooling speeds of steel greater than the cooling speed at which the ferrite is formed. Consequently, pearlite has a high level of stress; it is less stable thermodynamically than ferrite. In his study, focused on the localized corrosion behavior of reinforcement steel in simulated concrete pore solution, Zhang reported that the localized corrosion occurs on the ferrite grain boundaries and pearlite grains.[24]

Figure 3 shows the micrograph of a rusted sample. From this figure, we see clearly that the thickness of the oxide (rust) layer is not uniform and varies up to 0.046 mm.

B. *Corrosion Potential Evolution*

The corrosion potential (E_{corr}) is a qualitative indicator of the corrosion state of a metallic substrate in its environment. The evolution of the corrosion potential of the sample over time can follow the development of the steady state. It can also reveal the possible transitions from an active to a passive state of metal.

The effect of surface conditions of steel samples on the evolution of corrosion potential in SCP solution without and with chloride content is reflected by the curves of Figures 4(a) and (b). From these curves, we can see clearly the effect of the rust layer on the potential evolution of reinforcement steel.

At the beginning of their immersion in SCP solution free of chlorides, the rusted sample shows the highest potential value (+80 mV_{SCE}), while the polished sample gives the lowest (–580 mV_{SCE}). However, the potential

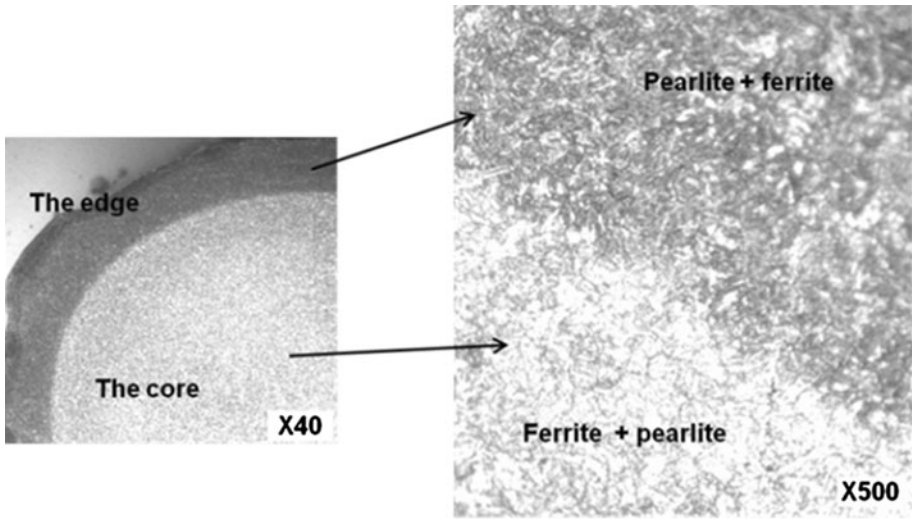

Fig. 2—Optical micrograph of polished sample.

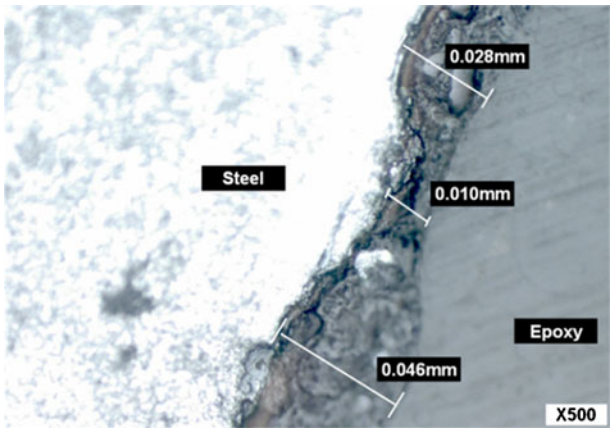

Fig. 3—Optical micrograph of rusted sample.

of the polished sample is increasingly positive with time, stabilizing around a value of –390 mV, while the potential of the rusted sample becomes more negative, stabilizing to a value of –380 mV.

In the presence of chlorides, the evolution of corrosion potential with time follows the same tendency for both kinds of samples (with and without rust). The potential becomes increasingly less noble with time and reaches values more negative than that achieved in chloride-free solution, which reflects the aggressive effect of chloride ions.

As a first conclusion, concerning the effect of the rust, we can say that, in the absence of chlorides, the rust provides to the steel bar a relative electrochemical stability. In the presence of chloride, however, the rust has a negative effect on the electrochemical behavior of reinforcement steel.

C. *Polarization Curves*

The use of polarization curves is very limited due to its destructive nature. However, it is possible to obtain important information on the kinetics of the corrosion reactions. Figures 5(a) and (b) show the anodic polarization curves obtained in SCP solution for steel samples with different surface conditions, metallurgically polished and rusted, respectively. From these curves, we can make the following observations.

For all the curves, we can see clearly the existence of a passivation plateau on the anodic branch before reaching the onset of the oxygen evolution reaction. This plateau is generally attributed to the formation of a passive film well adherent to the metal surface.

However, we observe that the effect of the surface conditions is quite clear and resides in the difference in the corrosion and passivation current densities and the potential at which the oxygen evolution reaction occurs. The lowest values of corrosion current (i_{corr}) and passivation current (i_{pass}) are given by the polished sample, while the highest values are given by the rusted sample. However, the lowest values of potential at which the oxygen evolution reaction occurs are obtained with the rusted sample.

In the presence of chloride ions, passivity breakdown occurred. For both specimens, the current density showed a higher increase, the corrosion potential took more negative values, and the pitting potential values were distinguished. Therefore, the steel in the SCP solution with 3 pct NaCl was unstable due to the chloride attack (pitting corrosion), as shown in Figure 6.

The values of the corrosion current density and corrosion potential given by the polished sample are lower than those given by the rusted sample, which reflects the negative effect of oxides on the corrosion behavior of reinforcement steel.

In brief, the results obtained from polarization curves are in agreement with those obtained from the evolution of corrosion potential with time. In fact, they confirm the negative effect of rust on the electrochemical behavior of reinforcing steel in simulated concrete solution especially in the presence of chloride ions. Table II gives the values of some electrochemical settings reflecting this effect.

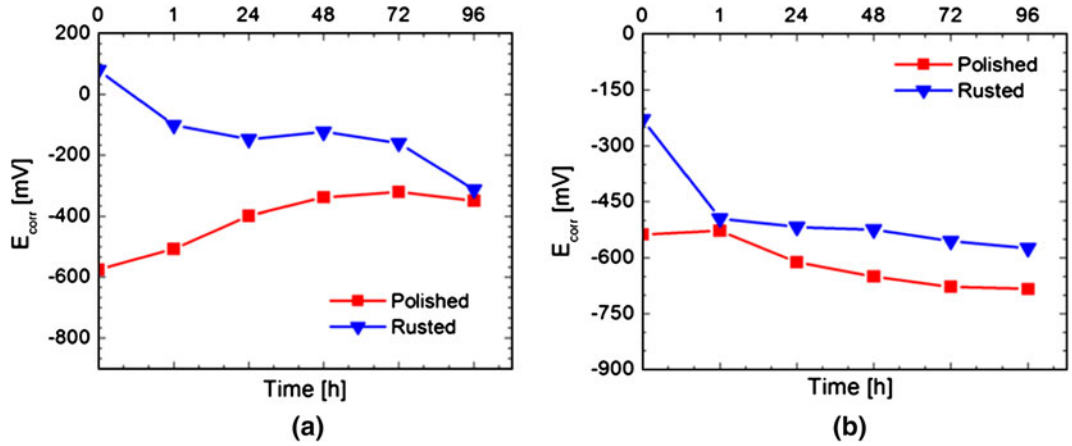

Fig. 4—Effect of surface conditions on the corrosion potential evolution of steel in SCP solution: (*a*) without chlorides and (*b*) with 3 pct chlorides.

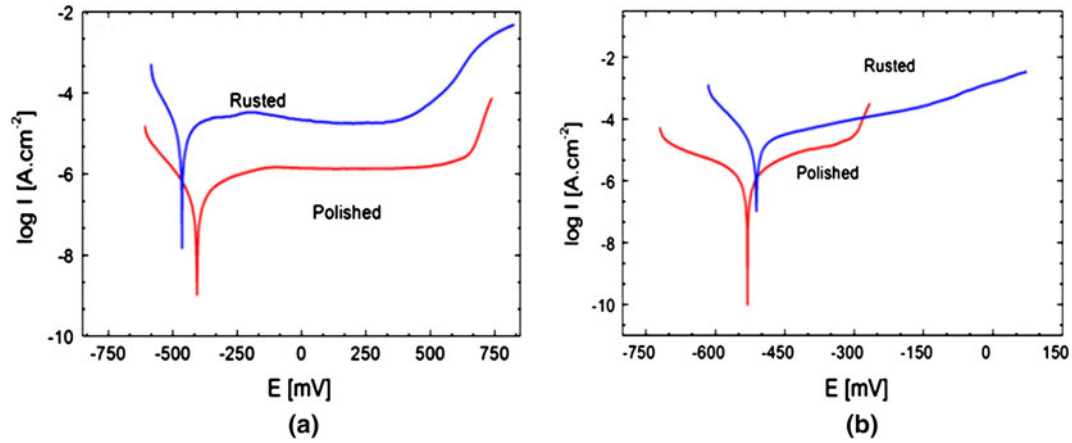

Fig. 5—Effect of surface conditions on the corrosion behavior of steel in SCP solution: (*a*) without chlorides and (*b*) with 3 pct chlorides.

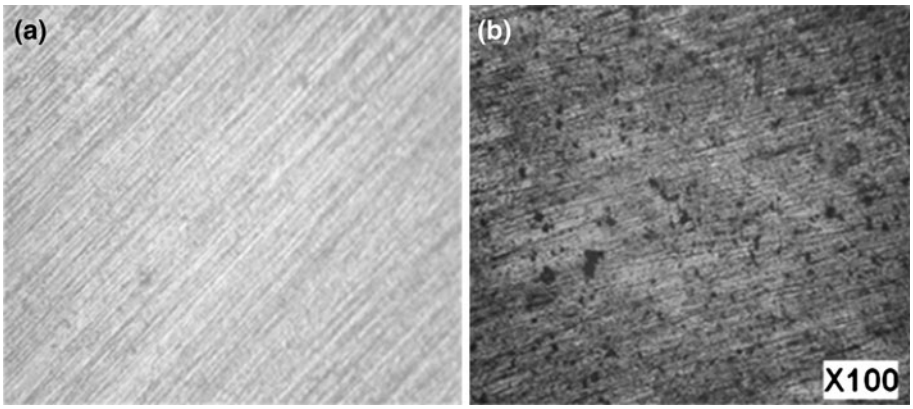

Fig. 6—Pitting corrosion causes by chloride attack for polished sample: (*a*) chloride-free solution and (*b*) chlorinated solution.

D. *Electrochemical Impedance Spectroscopy*

Figures 7(a), 7(b), 8(a), and 8(b) show the EIS diagram of steel specimens with the polished surface and rusted surface immersed in the SCP solutions for different times with and without chlorides.

The simulating equivalent circuit is represented in Figure 9, where R_0 is the solution resistance and R_1 is the interfacial charge transfer resistance. The nonideality of the surface of the electrode was considered by the inclusion of constant phase elements (CPE) instead

pure capacitors. Its impedance Z_{CPE} is defined as follows:

$$Z_{CPE} = [Y(j\omega)^n]^{-1} \quad [1]$$

where Y is a parameter with dimensions of Ω^{-1} cm^{-2} s^n, which is directly proportional to the double layer capacitance of pure capacitive electrodes; ω is the angle frequency in radians per second; and n represents the deviated degree of the capacitance of the solid electrode double-layer from the ideal condition, which is generally attributed to the inhomogeneity of the double-layer electric field.[12] The meaning of the parameters of the CPE depends on the n values ($0 \le n \le 1$). An ideal capacitor corresponds to $n = 1$, while $n = 0.5$ becomes the CPE in a Warburg component. The intermediate n value was related to the nonhomogeneities and the electrode surface roughness.[25] The fitting data of the corresponding elements in the equivalent circuit are listed in Tables III and IV.

Table II. Rust Effect on the Evolution of the Corrosion and Pitting Potential

	Cl^- (Pct)	E_{corr} (mV)	E_p (mV)
Polished surface	0	–406.5	630
	3	–530	–307
Rusted surface	0	–464.6	—
	3	–566	—

As can be seen, the impedance spectra of the reinforcing steel in the SCP solutions contain semicircles due to a time constant of the reactions taking place on the steel surface. The arc, which appeared at frequencies below 50 KHz, resulted from an interfacial reaction involving two processes with a similar and inseparable time constant. These processes were attributed to the electrochemical reaction on the electrode (film) surface and the associated charge transfer resistance and double-layer capacitance.[8] The consensus in the literature is that this passive film is extremely resistant to corrosion attack due to the high pH of the pore solution. However, the radii of capacitive semicircles for the steel in the chloride-free SCP solution increased with the immersion time, which means an increase of the impedance of the steel/electrolyte interface.

On the other hand, the radii of capacitive semicircles for steel in the SCP solution containing 3 pct NaCl decreased with the immersion time, indicating that the steel could not retain its passivity with the presence of chloride ions. The preceding trend could be further

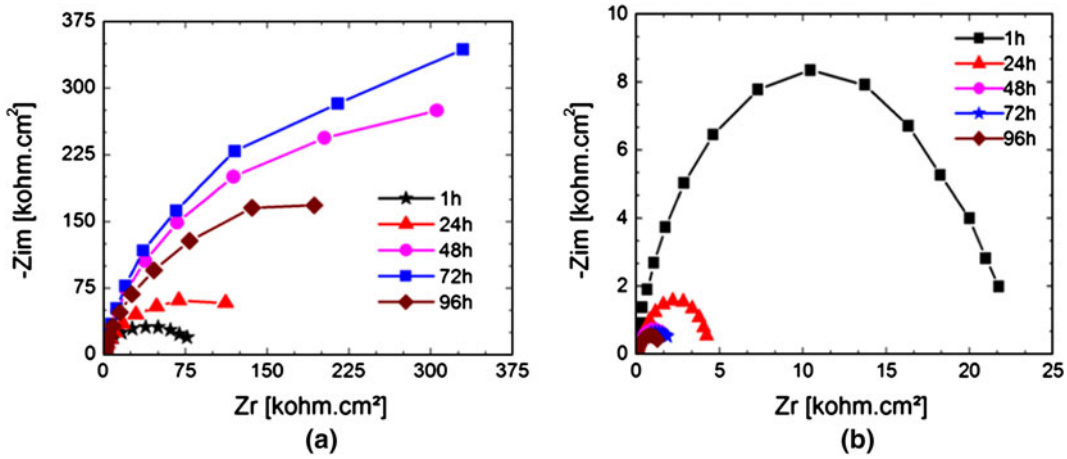

Fig. 7—Nyquist plot of reinforcement steel samples with polished surface: (*a*) without chlorides, (*b*) with 3 pct chlorides.

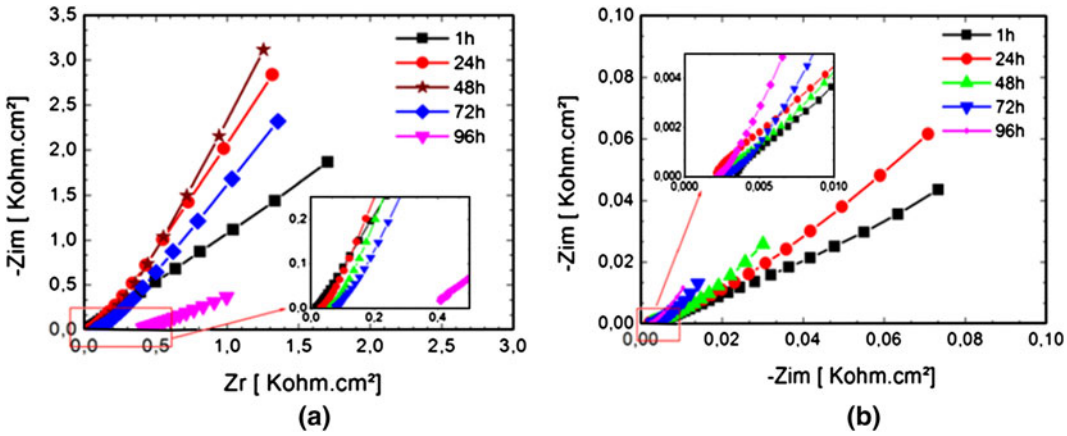

Fig. 8—Nyquist plot of reinforcement steel samples with rusted surface: (*a*) without chlorides and (*b*) with 3 pct chlorides.

supported by the quantified resistance values, as can be seen from the fitting data of R_1 in Tables III and IV. It is certain that the steel was stable in the chloride-free SCP solution, because the R_1 values increased quickly with the immersion time. The steel in the SCP solution with 3 pct NaCl was unstable and the corrosion might take place on its surface, as indicated by the decrease of the R_1 with immersion time.

Furthermore, the effect of chloride ions on the steel corrosion behavior can also be seen from the changes of Y. When a metal electrode is immersed in an aqueous solution, an electric double layer is established very rapidly. Generally, the model used to describe the electric double layer at the metal/solution interface is the simple capacitor.[12] Therefore, the CPE parameters Y and n can reflect the change of a reinforcing steel electrode surface relating to the oxide film formation. A number of studies have shown that the CPE parameters Y and n vary with the homogeneity of the electrode surface, with larger values of Y and smaller values of n being characteristic of more inhomogeneous surfaces. As shown in Tables III and IV, the effect of chloride ions on all the samples can also be seen from the changes in Y. In the chloride-free SCP solution, Y decreased slightly with the immersion time, and the n value was close to 1, indicating that the steel surface became more uniform and the oxide layer at the steel-solution interface was basically in keeping with the parallel-plate model of the capacitance, which could be interpreted as a passive film formation on the steel surface. However, the Y value slightly increased in the SCP solution containing chloride ions with the immersion time, which means that there was a gradual breakdown of the passive film with the presence of chloride ions, and the steel surface became rougher resulting from the occurrence of the steel corrosion. The n values could reflect the change of the steel electrode surface. By and large, the n value remained constant during the immersion process of steel in the same SCP solution. However, it was closer to one in the chloride-free solution, which means that the double layer in the steel/electrolyte interface tends toward a capacitance behavior, and the steel surface is then more homogeneous. The lower n values for the solution with 0.5M NaCl show that the steel surface becomes more inhomogeneous due to the chloride attack; hence, the steel can be corroded.

As presented in Tables III and IV, it is worth noting that Y had close values in a solution for different immersion times, but the value changes showed a certain evolution in relation to the interface changes. Thus, Y is an important parameter for evaluating the physicochemical

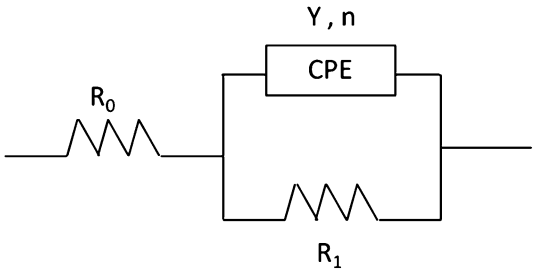

Fig. 9—Simulating equivalent circuit.

Table III. Fitting Results of EIS Circuit for Steel Samples with Polished Surface

	Time (h)	R_0 (Ohm)	$Y\ 10^{-5}$ (S s^n)	n	$C_{dl}\ 10^{-5}$ (F)	$R_1\ 10^4$ (Ohm)	Error in Z (Pct)
0 pct Cl^-	01	120.9	2.92	0.88	1.32	8.03	2.89
	24	226.6	2.36	0.87	1.08	1.49	3.13
	48	321.5	1.96	0.89	1.086	6.34	0.94
	72	424	1.87	0.90	1.07	8.09	2.97
	96	1009	2.00	0.89	1.26	4.14	1.83
3 pct Cl^-	01	11.55	4.64	0.85	1.27	2.15	3.07
	24	10.55	1.96	0.74	2.23	4.57	5.49
	48	9.43	6.10	0.71	7.63	2.30	5.66
	72	10.47	6.46	0.74	11.34	1.65	2.91

Table IV. Fitting Results of EIS Circuit for Steel Samples with Rusted Surface

	Time (h)	R_0 (Ohm)	$Y\ 10^{-5}$ (S s^n)	n	$C_{dl}\ 10^{-5}$ (F)	$R_1\ 10^4$ (Ohm)	Error in Z (Pct)
0 pct Cl^-	01	16.23	0.001789	0.5283	7.58	3.9×10^{13}	4.89
	24	35.77	0.00205	0.6254	42.87	2.9×10^{13}	12.08
	48	66.25	0.002045	0.6513	70.13	3.2×10^{13}	11.47
	72	85.46	0.002132	0.5929	66.23	3.2×10^{11}	8.73
	96	3.81×10^5	3.52×10^{-7}	0.3341	6.44	1.1×10^{16}	0.61
3 pct Cl^-	01	3	0.03	0.3	10.89	1.5×10^{12}	2.78
	24	1.87	0.031	0.35	15.65	1.9×10^{12}	8.3
	48	2.49	0.074	0.344	294	1.2×10^{10}	8.6
	72	2.85	0.193	0.41	8160	7.9×10^{10}	8.25

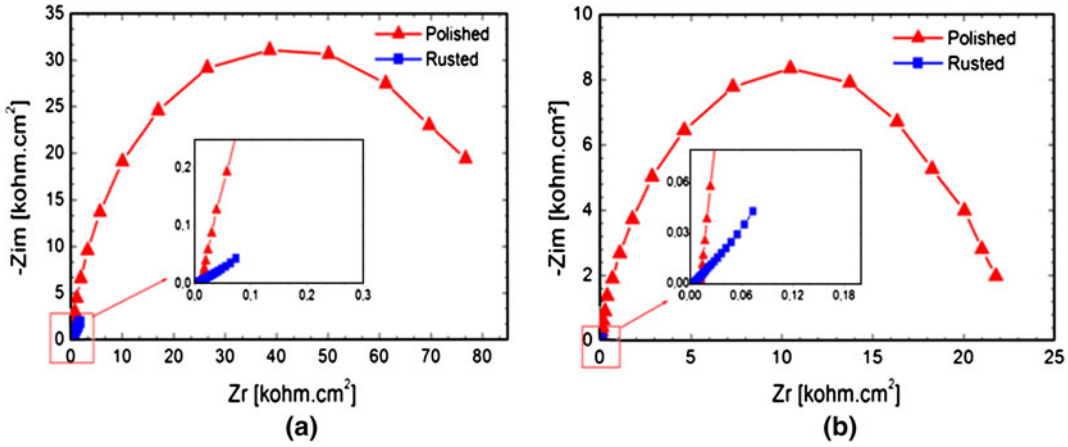

Fig. 10—Nyquist plots of the effect of surface conditions on the corrosion behavior of steel in CPS without and with chlorides after 1 h: (*a*) without chlorides and (*b*) with 3 pct chlorides.

characteristics of the steel/solution interface related to the corrosion behavior of the material. However, R_0 does not depend on the process or corrosion products, but only on the concentration of Cl^- ions in solution.

The impedance spectra reflecting the surface conditions' effect on electrochemical behavior of reinforcement steel in SCP solutions are shown in Figures 10(a) and (b). From these spectra, we can see clearly the detrimental effect of rust on the corrosion behavior of steel, especially when the solution is chlorinated. This effect is reflected by a significant reduction in size of the impedance arc. Therefore, an increase in the capacity of the double layer (C_{dl}) and a decrease of polarization resistance (R_p) of rusted samples are observed. This means that when the charge transfer is high, the surface of the material is more active.

E. *Discussion*

The obtained results show that the corrosion rate of rebar is greater in the presence of chlorides. Chloride ions have two effects on the corrosion mechanisms: (1) they increase the ionic conductibility of the electrolyte, which facilitates the transport of ions; and (2) they provoke localized breakdown of the passive layer. At sites where the layer was destroyed, the steel dissolution occurred (anodic sites), while the surfaces that remained passive corresponded to the cathodic sites. Hence, the high ratio of cathode/anode promotes the localized and in-depth progress of corrosion. The mechanism of this kind of corrosion is too complex, because the composition of the solution within the pit is changed compared to the interstitial solution that surrounds it. In the pitting, the chloride ions react with hydrogen ions from water to form hydrochloric acid, as follows:

$$Fe^{2+} + Cl^- + H_2O \rightarrow FeOH^+ + HCl \quad [2]$$

$$HCl \rightarrow Cl^- + H^+ \quad [3]$$

These reactions cause a significant drop of pH solution in the pit.[26] The dissolution of iron is accelerated. The regenerated chloride ions continue to be active during the corrosion process, which becomes thus an autocatalytic process. Hydroxyl ions in the interstitial solution are then combined with the Fe^{2+} ions that diffuse outside the pitting, while the cathodic reaction is the same as in the case of corrosion in the absence of chlorides.

$$Fe^{2+} + 2OH^- \rightarrow Fe(OH)_2 \quad [4]$$

$$H_2O + 1/2O_2 + 2e^- \rightarrow 2OH^- \quad [5]$$

Active corrosion of rusted steel can be explained as follows: the presence of rust hinders the process of passivation of the metal due to the high alkalinity of the concrete pore solution; therefore, rust acts as a physical barrier against the diffusion of hydroxyl ions toward the surface of the steel.

The polished steel samples present a corrosion product forming a beneficial barrier layer called the "passive layer" ($Fe(OH)_2$), while the prerusted steel is susceptible to localized corrosion (presence of cathodic areas [oxides] and anodic areas [where the oxide layer is locally destroyed]). These defects (local destruction of the oxide film) are privileged sites for the attacks in depth of the metallic matrix; the cathodic surface is much larger than the anode surfaces (local film defects), causing faster development of pitting corrosion evolving to a crevice corrosion form. The reduction of the steel section and, therefore, its load capacity can lead to catastrophic failure.

The four main phases constituting the rust layer are goethite (α-FeOOH), lepidocrocite (γ-FeOOH), magnetite (Fe_3O_4), and hematite (α-Fe_2O_3). Akaganeite (β-FeOOH) can be linked with the presence of chlorides in the environment.[25] The former is the predominant phase in the composition of unaged rust formed in relatively short exposure times and is also usually the only reactive compound of the rust. Once it appears, the

akaganeite can play a fundamental role in the corrosion process. It is noted that the polarization of rust to negative potentials causes the formation of Fe^{2+} states in the oxide lattice, which confer an electrical conductivity to the oxide. This parameter is necessary for the continuity of the electrochemical process between the local anodes in the metal and the local cathodes in the surrounding rust. In general, the final composition of the reduced rust depends to a great extent on the pH, polarization potential, and composition of the electrolyte.

The strong tendency of prerusted steel to develop active corrosion results in a direct relation between the corrosion rate and the amount of rust initially present on the steel surface. This rust favors corrosion both by providing a reducible material for the cathodic reaction and by acting as a porous electrode for the reduction of oxygen.[19]

IV. CONCLUSIONS

The obtained results show that the presence of rust on the reinforcement surface has a negative effect on its corrosion behavior, with or without chlorides.

The rust effect on the corrosion behavior is expressed by a significant increase in the corrosion current density and a decrease in polarization resistance and pitting potential. Also, the obtained EIS spectra confirm this negative effect by showing that the presence of rust leads to a reduced total impedance of the system.

The presence of rust in the steel surface provokes a decrease of the electrolyte resistance at the metal-concrete interface and reduces the repassivating ability. On the other hand, the rust layer acts as a barrier against the ions' hydroxyl diffusion, which prevents the realkalinization phenomenon.

REFERENCES

1. V. Feliu, G.A. Gonzalez, and S. Feliu: *J. Appl. Electrochem.*, 2005, vol. 35, pp. 429–36.
2. O. Poupard, A. Aït-Mokhtar, and P. Dumargue: *Cem. Concr. Res.*, 2004, vol. 34, pp. 91–1000.
3. G. Batis and E. Rakanta: *Cem. Concr. Compos.*, 2005, vol. 27, pp. 269–75.
4. F.G. da Silva and J.B. Liborio: *Mater. Res.*, 2006, vol. 9, pp. 209–15.
5. B. Huet, V. L'hostis, F. Miserque, and H. Idrissi: *Electrochim. Acta*, 2005, vol. 51, pp. 172–80.
6. U. Angst, B. Elsener, C.K. Larsen, and O. Vennesland: *J. Appl. Electrochem.*, 2010, vol. 40, pp. 561–73.
7. L. Dhouibi, Ph. Refait, E. Triki, and J. Génin: *J. Mater. Sci.*, 2006, vol. 41, pp. 4928–36.
8. M. Saremi and E. Mahallati: *Cem. Concr. Res.*, 2002, vol. 32, pp. 1915–21.
9. J. Bonastre, P. Garcés, F. Huerta, C. Quijada, L.G. Andión, and F. Cases: *Corros. Sci.*, 2006, vol. 48, pp. 1122–36.
10. T. Henriques, A. Reguengos, L. Proença, E. Pereira, M. Rocha, M. Neto, and I. Fonseca: *J. Appl. Electrochem.*, 2010, vol. 40, pp. 99–107.
11. N. Birbilis, K.M. Nairn, and M. Forsyth: *Electrochim. Acta*, 2004, vol. 49, pp. 4331–39.
12. W. Chen, D. Rong-Gui, Y. Chen-Qing, Z. Yan-Feng, and L. Chang-Jian: *Electrochim. Acta*, 2010, vol. 55, pp. 5677–82.
13. H. Tamura: *Corros. Sci.*, 2008, vol. 50, pp. 1872–83.
14. M. Yamashita, H. Miyuki, Y. Matsuda, H. Nagano, and T. Misawa: *Corros. Sci.*, 1994, vol. 36, pp. 283–99.
15. E. Zitrou, J. Nikolaou, P.E. Tsakiridis, and G.D. Papadimitriou: *Constr. Build. Mater.*, 2007, vol. 21, pp. 1161–69.
16. A.J. Al-Tayyib, M. Shamin Khan, I.M. Allam, and A.I. Al-Mana: *Cem. Concr. Res.*, 1990, vol. 20, pp. 955–60.
17. E. Proverbio and R. Cigna: *Mater. Sci. Forum,* 1995, pp. 877–82.
18. C.M. Hanson and B. Sorensen: "Corrosion Rates of Steel in Concrete," ASTM STP 1065, ASTM, Philadelphia, PA, 1990.
19. J.A. González, J.M. Miranda, E. Otero, and S. Feliu: *Corros. Sci.*, 2007, vol. 49, pp. 436–48.
20. L.T. Mammoliti, L.C. Brown, C.M. Hansson, and B.B. Hope: *Cem. Concr. Res.*, 1996, vol. 26, pp. 545–50.
21. P. Novak, R. Mala, and L. Joska: *Cem. Concr. Res.*, 2001, vol. 31, pp. 589–93.
22. M. Maslehuddin, M.M. Al-Zahrani, S.U. Al-Dulaijan, Abdulquddus, S. Rehman, and S.N. Ahsan: *Cem. Concr. Compos.*, 2002, vol. 24, pp. 151–58.
23. J.A. González, A. Bautista, and S. Feliu: *Cem. Concr. Res.*, 1996, vol. 6, pp. 501–11.
24. F. Zhang, J. Pan, and C. Lin: *Corros. Sci.*, 2009, vol. 51, pp. 2130–38.
25. M. Keddam, H. Takenouti, X.R. Nóvoa, C. Andrade, and C. Alonso: *Cem. Concr. Res.*, 1997, vol. 27, pp. 1191–1201.
26. D. Landolt: *Corrosion et Chimie de Surfaces des Métaux*, Presse Polytechniques et Universitaires Romandes, Lausanne, Switzerland, 2003.